

Minimisation of Required Charge for Desired Neuronal Spike Rate

Craig O. Savage^{♥,1,2}
Anthony N. Burkitt^{1,2,3,4}

Tatiana Kameneva^{1,2}

David B. Grayden^{1,2,3,4}

Hamish Meffin^{1,3}

Abstract—Retinal implants restore limited visual perception to blind implantees by electrical stimulation of surviving neurons. We consider the efficacy of two electrical stimulation parameters, frequency of stimulation and interphase gap between cathodic and anodic phases, on the required charge to reach a desired neuronal spike rate. Using a Hodgkin-Huxley model of a neuron, we find the most efficient means of achieving a desired spike rate for neurons by electrical stimulation is to use a stimulation frequency identical to the desired spike rate, as well as a long interphase gap.

I. INTRODUCTION

Retinitis pigmentosa is a condition causing retinal degeneration. This generation results in the death of photoreceptors (i.e., rods and cones), thereby breaking the chain between light received by the eye, and signals transmitted to the brain. However, some of the retinal ganglion cells (RGCs), which are neurons found in the eye, may survive after the death of photoreceptors [1]. Retinal implants aim to restore sight by providing direct electrical stimulation to these surviving RGC, thereby restoring a level of sight. Electrical stimulation generating visual perception has been known for over 75 years [2], but controlling perception via electrical stimulation is an active area of research. Such controlled stimulation has been shown to enable differentiating the direction of lines, recognising letters, and identifying common objects (e.g., words) [3], [4]. There have been perceptual models relating electrical stimulation to implantee perception, as well as *in vitro* and *in vivo* studies regarding retinal response to electrical stimulation.

The RGCs communicate information to the brain via electrical spikes. Tests have been performed on the impact of different electrical stimulation parameters to elicit a spike from a RGC with a given probability (frequently 50%). This threshold stimulus may be lowered by modifying electrical stimulation parameters.

Inclusion of an interphase gap (hereafter, IPG) has been shown to lower thresholds for cochlear implants [5], and in an animal model for retinal implants [6]. In contrast, we are interested in achieving a desired spiking rate, rather than exceeding some spiking threshold. An advantage to employing an IPG to a stimulation waveform is that it does

not increase the required charge, power, or other electrical requirements of the stimulation.

One way to control neuronal spike rate is to stimulate with pulses at different frequencies. It is possible to elicit one spike per pulse [7]. Here, there is a trade-off to induce a spike: higher current amplitudes result in larger probabilities of spiking on a given pulse, but more pulses at lower current may produce the same expected number of spikes.

II. METHODS

A previously constrained model of an OFF RGC was used for simulations [8]. A single-compartment Hodgkin-Huxley-type neuron was simulated in NEURON. The membrane potential, V , changed with time, t , according to:

$$C_m \frac{dV}{dt} + I_{Na} + I_{Ca} + I_{K,A} + I_{K(Ca)} + I_K + I_T + I_h + I_{NaP} + I_L + I_{Stim} = 0, \quad (1)$$

where C_m is a specific membrane capacitance. Sodium, I_{Na} , L-type calcium, I_{Ca} , potassium, $I_{K,A}$, $I_{K(Ca)}$, I_K , low-voltage activated T-type calcium, I_T , hyperpolarization-activated, I_h , sodium-persistent, I_{NaP} , and leak, I_L , currents were constrained as discussed in other studies [8], [9], [10], [11]. I_{Stim} is an intracellular stimulation current that is described below.

In our simulation, a standard Euler integration method was used with a time step of 0.025ms. All voltage-dependent parameters were initialized at a membrane potential of $-65mV$.

The model of RGCs was used to investigate the effect of electrical stimulation. It was assumed that stimulation current that passes across the membrane, I_{Stim} in (1), is proportional to the current being passed through the extracellular stimulation electrodes. An intracellular stimulation current, I_{Stim} , was a symmetric bi-phasic current injection as shown in Figure 1. Duration of the cathodic and anodic phases, ω_+ and ω_- , were set to 0.095ms similar to [7]. To explore the responses of the model neurons to trains of pulses of different frequencies, amplitudes and interphase gaps, the following parameters were varied in simulations. The amplitude of the cathodic and anodic phases, A_+ and A_- , were varied from 0.2nA to 0.5nA with a linear step size of 0.003nA. The IPG, Δ , was varied from 0 to 0.975ms with a linear step size of 0.1625ms. Frequency of the pulse train stimulation, f_s , was varied from 20 to 100Hz with a linear step size of 20Hz. The parameter space of the IPG duration and frequency of pulse train stimulation was systematically explored with stimulations of an OFF RGC.

¹ NeuroEngineering Laboratory, Department of Electrical and Electronic Engineering, The University of Melbourne, VIC 3010 Australia. ² Centre for Neural Engineering, The University of Melbourne, VIC 3010 Australia. ³ NICTA Victoria Research Labs, The University of Melbourne, VIC 3010 Australia. ⁴ Bionics Institute, 384-388 Albert St, East Melbourne, VIC 3002 Australia. ♥: Correspondence to be sent to: cosavage@unimelb.edu.au

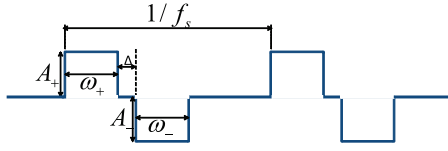


Fig. 1. Stimulation waveform used in this work. The current magnitude, a , and interphase gap, Δ , are controlled. Two pulse pairs are shown here, and pulses are repeated at 20–100Hz (i.e., the time between leading edges varies from 50–10ms).

III. RESULTS

In this section, we present results showing the minimum required charge to reach a desired neuronal spike rate. We also estimate the probability of a neuron spiking as the number of spikes predicted divided by the stimulation frequency.

Figure 2 gives a probability of eliciting a spike from a single pulse pair stimulation. This gives us a normalised measure to determine the efficacy of our stimulation pulses as a function of current magnitude and interphase gap. As shown in Figure 2, at an amplitude below threshold, a spike is not elicited from a single pulse stimulation. An example of such a response is given in Figure 3a for $\Delta = 0.975\text{ms}$, $f = 100\text{Hz}$ and $|A_+| = |A_-| = 0.3\text{nA}$. In comparison, with stimulation amplitude $|A_+| = |A_-| = 0.4$, a spike is elicited at each pulse stimulation (Figure 3b).

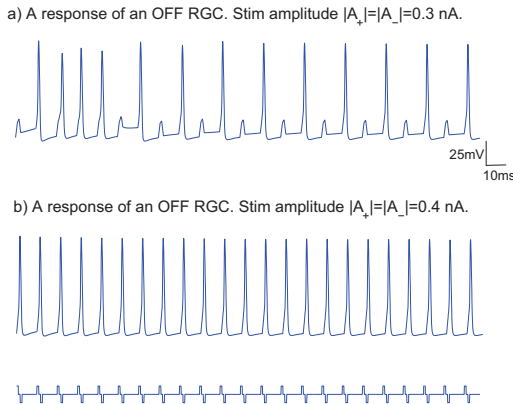


Fig. 3. Modelled neuronal spiking activity resulting from electrical stimulation. The top part of each plot shows spikes, while the lower shows the biphasic stimulation waveform applied (I_{stim}). Each stimulation is at 100Hz for 500ms, with an IFG of 0.975ms.

In Figure 4, we present the amount of total charge required in the stimulation phase to elicit a desired spike rate at different stimulation rates for the longest studied IPG, as they result in lower required currents for eliciting a desired spiking rate (see Figure 2). The total charge is calculated assuming a 1sec stimulation duration, and is given by

$$Q = f_s A_+ \omega_+ \times 1\text{sec}, \quad (2)$$

where f_s represents the stimulation frequency (depicted as different lines in the figure), A_+ represents the current

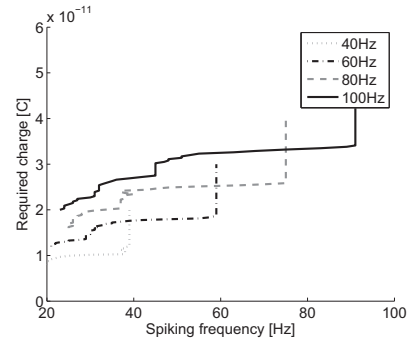


Fig. 4. Required charge to reach a target spike rate for different stimulation rates. In each case, there is an interphase gap of $\Delta = 0.975\text{ms}$.

magnitude (implicitly in the desired spike rate along the x -axis), and $\omega_+ = 0.095\text{ms}$ is the pulse width.

Each line in Figure 4 has limited extent, to the limit of one-spike-per-stimulation; for example, the 40Hz line projects to the 40Hz spike rate. For better visualization, we didn't include data for a 20Hz stimulation frequency as it barely enters the graph. Plots for other values of IPG are similar, albeit shifted upwards in terms of the total charge required.

IV. DISCUSSION

We have shown that an increasing interphase gap leads to a decrease in the charge required to cause a neuron to spike. Another way of viewing this is that an increasing interphase gap results in a larger probability of neuronal firing. This result occurs for all tested frequencies of stimulation.

Note that this is a separate result from a lower threshold as in previous studies; instead we have a desired spike rate and are trying to reach it, rather than a single spike some percentage of the time. Comparable literature on impacts of thresholds includes electrode size [12], single phase pulse duration [13], [14], first pulse polarity [15], [16], distance from the stimulating electrode to the retinal surface [17], and interphase gap [6].

Referring to the graphs in Figure 2, saturation trends emerge, with plateaus of neuron response predicted. For example, at 20Hz stimulation, the rise to one spike per stimulation pulse is rapid in both interphase gap and applied current. Conversely, at 40Hz stimulation, more current is required to reach a probability of spiking of 0.5 than saturation at 20Hz. Hence, to efficiently elicit a 20Hz spike rate, it is optimal (in sense of minimal required charge) to stimulate with a lower frequency. Coupled with an experimentally observed result that with the direct stimulation of RGCs one spike is elicited per pulse, even at higher rate of stimulation, [7], we propose that to elicit a given spike rate, f_D , one should stimulate at that rate. Hence, $f_s = f_{\text{Desired}}$ appears optimal in terms of minimal charge required.

There are steep sections of the neuronal response curves, with plateaus of near-constant neuronal response between them. Based on these graphs, the response of a given waveform as a function of current might be best represented as a double logistic function rather than a single sigmoid. As

an example, we consider stimulation at different rates at the extrema of interphase gaps (i.e., $\Delta = 0\text{ms}$ and 0.975ms), as shown in Figure 5.

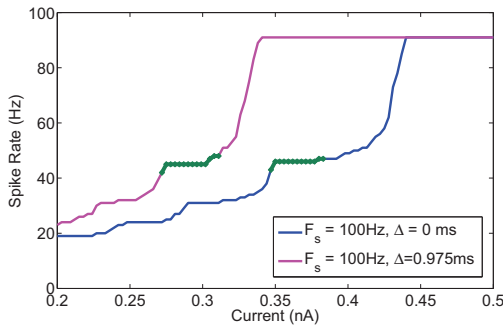


Fig. 5. Neuronal spike rate in response to stimulation at 100Hz for the extreme values of IPG considered in this work. Plateaus of spike rates at different current magnitudes are highlighted. Although the current regime has shifted upon introduction of a long IPG, the plateau at a response of $\sim 50\text{Hz}$ occurs in both sets of stimulation (highlighted in green). Conversely, a longer plateau is observed in the case of no IPG at $\sim 20\text{Hz}$ that is not apparent over our range of current amplitudes if a long IPG is employed.

These plateaus may have implications for users of retinal implants. From the point of view of the device, larger currents are necessary to overcome these plateaus and reach higher spike rates. However, selected stimulation amplitude within a plateau may yield consistent perception of the implantee, as the neuronal spike rate is constant over a range of current magnitude, yielding robustness to deviations in delivered current.

Finally, we must acknowledge that our simulations are based upon a model of *intracellular* stimulation, whereas current retinal implants provide *extracellular* stimulation. Indeed, the current magnitudes predicted to elicit spike rates are smaller than those found in the literature [12], [3], [18], [19].

V. ACKNOWLEDGMENTS

This research was supported by the Australian Research Council (ARC) through its Special Research Initiative (SRI) in Bionic Vision Science and Technology grant to Bionic Vision Australia (BVA). The Bionics Institute acknowledges the support it receives from the Victorian Government through its Operational Infrastructure Support Program.

REFERENCES

- [1] N. E. Medeiros and C. A. Curcio, "Preservation of ganglion cell layer neurons in age-related macular degeneration," *Investigative Ophthalmology & Visual Science*, vol. 42, no. 3, pp. 795–803, 2001.
- [2] H. Barlow, H. Kohn, and E. Geoffrey Walsh, "Visual sensations aroused by magnetic fields," *American Physiological Society*, vol. 148, no. 2, pp. 372–375, 1947.
- [3] M. Humayun, J. Weiland, G. Fujii *et al.*, "Visual perception in a blind subject with a chronic microelectronic retinal prosthesis," *Vision Research*, vol. 43, no. 24, pp. 2573–2581, 2003.
- [4] E. Zrenner, R. Wilke, K. Bartz-Schmidt, H. Benav, D. Besch, F. Gekeler, J. Koch, K. Porubsk, H. Sachs, and B. Wilhelm, "Blind retinitis pigmentosa patients can read letters and recognize the direction of fine stripe patterns with subretinal electronic implants," vol. 50, pp. E-Abstract 4581, 2009.

- [5] R. Shepherd and E. Javel, "Electrical stimulation of the auditory nerve: II. Effect of stimulus waveshape on single fibre response properties," *Hearing Research*, vol. 130, pp. 171–188, 1999.
- [6] A. C. Weitz, M. R. Behrend, M. S. Humayun, R. H. Chow, and J. D. Weiland, "Interphase gap decreases electrical stimulation threshold of retinal ganglion cells," in *Proceedings of the 33rd Annual Engineering in Medicine and Biology Conference (EMBC)*, 2011, pp. 6725–6728.
- [7] S. I. Fried, A. C. W. Lasker, N. J. Desai, D. K. Eddington, and J. F. Rizzo, "Axonal sodium-channel bands shape the response to electric stimulation in retinal ganglion cells," *Journal of Neurophysiology*, vol. 101, no. 4, pp. 1972–1987, April 2009.
- [8] T. Kameneva, H. Meffin, and A. N. Burkitt, "Modelling intrinsic electrophysiological properties of ON and OFF retinal ganglion cells," *Journal of Computational Neuroscience*, vol. 3, pp. 547–561, 2011.
- [9] J. F. Fohlmeister and R. F. Miller, "Impulse encoding mechanisms of ganglion cells in the tiger salamander retina," *Journal of Neurophysiology*, vol. 78, no. 4, pp. 1935–1947, 1997.
- [10] X. J. Wang, J. Rinzel, and M. A. Rogawski, "A model of the t-type calcium current and the low-threshold spike in thalamic neurons," *Journal of Neurophysiology*, vol. 66, no. 3, pp. 839–850, 1991.
- [11] I. van Welie, M. W. H. Remme, J. A. van Hooft, and W. J. Wadman, "Different levels of ih determine distinct temporal integration in bursting and regular-spiking neurons in rat subiculum," *The Journal of Physiology*, vol. 576, no. 1, pp. 203–214, 2006.
- [12] C. Sekirnjak, P. Hottowy, A. Sher, W. Dabrowski, A. Litke, and E. Chichilnisky, "Electrical stimulation of mammalian retinal ganglion cells with multielectrode arrays," *Journal of Neurophysiology*, vol. 95, no. 6, pp. 3311–3327, 2006.
- [13] A. E. Grumet, J. L. W. Jr., and J. F. R. III, "Multi-electrode stimulation and recording in the isolated retina," *Journal of Neuroscience Methods*, vol. 101, no. 1, pp. 31 – 42, 2000.
- [14] D. Tsai, J. Morley, G. Suaning, and N. Lovell, "Direct activation and temporal response properties of rabbit retinal ganglion cells following subretinal stimulation," *Journal of Neurophysiology*, vol. 102, no. 5, pp. 2982–2993, 2009.
- [15] M. Abramian, N. H. Lovell, J. W. Morley, G. J. Suaning, and S. Dokos, "Activation of retinal ganglion cells following epiretinal electrical stimulation with hexagonally arranged bipolar electrodes," *Journal of Neural Engineering*, vol. 8, no. 3, p. 035004, 2011. [Online]. Available: <http://stacks.iop.org/1741-2552/8/i=3/a=035004>
- [16] R. J. Jensen and J. F. R. III, "Activation of retinal ganglion cells in wild-type and rd1 mice through electrical stimulation of the retinal neural network," *Vision Research*, vol. 48, no. 14, pp. 1562 – 1568, 2008.
- [17] Ralph J. Jensen and Joseph F. Rizzo, III, "Thresholds for activation of rabbit retinal ganglion cells with a subretinal electrode," *Experimental Eye Research*, vol. 83, no. 2, pp. 367 – 373, 2006.
- [18] A. Horsager, S. Greenwald, J. Weiland, M. Humayun, R. Greenberg, M. McMahon, G. Boynton, and I. Fine, "Predicting visual sensitivity in retinal prosthesis patients," *Investigative Ophthalmology & Visual Science*, vol. 50, no. 4, pp. 1483–1491, 2009.
- [19] C. de Balthasar, S. Patel, A. Roy, R. Freda, S. Greenwald, A. Horsager, M. Mahadevappa, D. Yanai, M. McMahon, M. Humayun, R. Greenberg, J. Weiland, and I. Fine, "Factors affecting perceptual thresholds in epiretinal prostheses," *Investigative Ophthalmology & Visual Science*, vol. 49, no. 6, pp. 2303–2314, 2008.

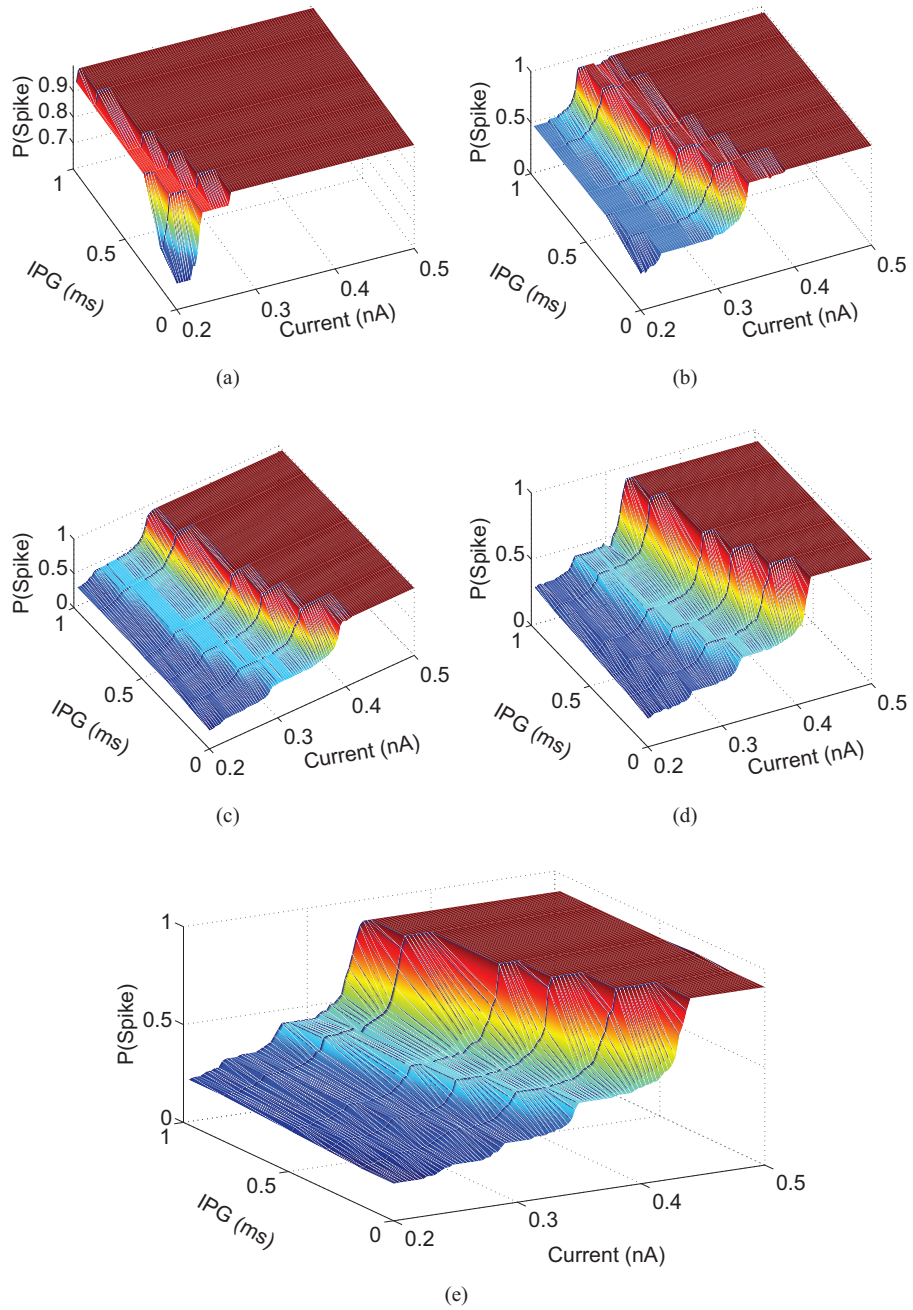


Fig. 2. Expected spikes from a single pulse pair stimulation for frequencies of 2(a) 20Hz, 2(b) 40Hz, 2(c) 60Hz, 2(d) 80Hz, and 2(e) 100Hz.